

Taking Full Advantage of RGB Sensor's Colorimetric Characteristics in Multi-Spectral Imaging

A. Mahmoudi Nahavandi

Department of Color Imaging and Color Image Processing, Institute for Color Science and Technology, P. O. Box: 16765-654, Tehran, Iran.

ARTICLE INFO

Article history:

Received: 30 Jul 2019

Final Revised: 7 Sept 2019

Accepted: 8 Sept 2019

Available online: 16 Oct 2019

Keywords:

Multispectral imaging

Optical filter

RGB camera

Spectral reconstruction.

ABSTRACT

Spectral images are the most valuable data than can be achieved using 2D sensors. Spectral estimation using data with a few channel cameras has been the subject of many studies. It is common to use color filters in front of the lens for increasing dimensionality of data. However, spectral estimations are prone to suffer from colorimetric errors. To address this problem it was shown that this problem is a special case of error-free spectral estimation problem. Considering the fact that most of RGB cameras tend to be colorimetric, using geometrical modeling of the problem, it was shown that adding a shoot with bare lens to the sensor's data can solve the problem. The notion has been tested in different scenarios and the efficiency of the proposed method has been proved in the scenarios. Results showed that if the camera is acceptably colorimetric, the proposed method can even leads to error-free colorimetric performance. *Prog. Color Colorants Coat. 13 (2020), 121-130* © Institute for Color Science and Technology.

1. Introduction

Digital cameras have revolutionized the photography industry. Images are taken within a few hundredths of seconds with software enabled correction capability. Unwanted shoots can easily be removed without the fear of spoiling one frame of raw negative stock. Despite this lovely simplicity for the users, there are troubles that the manufactures should overcome. One of the most important challenges is that these devices have to be colorimetric. Deviation from colorimetric behavior can cause objectionable wrong colors due to observer metamerism [1, 2].

Beside many reported color measurement applications, there is plethora of studies on spectral reflectance/radiance measurement using digital cameras. Regardless of using scientific or industrial digital cameras in these studies, the key concept is to increase the dimensionality of the image data with

adding a few more colored filters or shooting with more than one illumination condition [3-6]. These setups will change the RGB camera or scanner to spectral one, giving valuable spatial-spectral data of any sample. This technique has been utilized for making dream of spectral color management come true [7].

In addition to factory mounted color filters on the CMOS or CCD sensors, it is common to add more extra filters in front of camera lens. Filters can be added manually or automatically via a filter wheel. A conventional RGB camera equipped with 2 filters can give 6 channels from which spectral data can be estimated. Although adding filters to a RGB camera can increase the data dimensionality, it may deteriorate its inherent colorimetric characteristic due to rotation of sensor-filter-light vector subspace from eye-light subspace [2, 3]. That is, the color filter may decrease

colorimetric performance while enhancing spectral performance of the imaging system.

A practical necessity for resolving this problem is presented in this paper. The method is based on concurrent spanning of colorimetric and spectral subspaces. To do so, a brief review of the linear model of camera is presented in section 2. As sensitivity and noise of sensor enter into the estimator operator, a technique for estimation of camera sensitivity and intrinsic noise of sensor is studied in sections 3 and 4, respectively. Afterwards, using algebraic and geometrical modeling of the problem, the core idea of the paper is presented in section 5. Finally, the functionality of the proposed idea has been tested using sensitivities of a commercial RGB digital camera.

Throughout the paper, small lowercase letters denote scalars. Small boldface letters are used to indicate vectors and capital bold face letters are used for matrices. All of the matrices and the vectors are column wise.

2. Linear Model of Camera

CMOS and CCD sensors have an inherent characteristic to add the signals generated from different wavelengths. That is, for a polychromatic spectral signal, the camera response would be the sum of the responses for each wavelength. It seems as if camera signals are dot product of the spectral stimuli and the camera sensor sensitivities. So the well-known linear model of signal model has been used for modeling the camera as shown in Equation 1.

$$\mathbf{c} = \mathbf{W}^t \mathbf{L} \mathbf{r} + \mathbf{n} \quad (1)$$

where, \mathbf{c} is column vector of camera responses, \mathbf{W} shows the camera sensor sensitivity matrix, \mathbf{L} is a diagonal matrix with the light source radiance on its main diagonal, \mathbf{r} denotes the reflectance of a sample and the superscript t denotes transpose of a matrix. For simplicity, it is assumed that \mathbf{L} is combined with \mathbf{W} producing matrix \mathbf{W}_L . Assuming zero noise in the model, Equation 2 is rewritten as:

$$\mathbf{c} = \mathbf{W}_L^t \mathbf{r} \quad (2)$$

A wise criterion for estimation of \mathbf{r} from camera responses is to minimize the root mean square of estimation error for some selected \mathbf{r} s. It was shown that the linear operator that satisfies this criterion is the

well-known Wiener filter [8]. Wiener filter estimation is shown in Equation 3.

$$\hat{\mathbf{r}} = \mathbf{K}_r \mathbf{W}_L (\mathbf{W}_L^t \mathbf{K}_r \mathbf{W}_L + \mathbf{K}_n)^{-1} \mathbf{c} \quad (3)$$

Where \mathbf{K}_r and \mathbf{K}_n are covariance matrices of reflectance and noise, respectively, and $\hat{\mathbf{r}}$ is the estimation of reflectance using camera response \mathbf{c} .

As sensitivity and noise of the imaging system are prerequisites of Eq. 3, a brief review about estimation of sensitivities and noise of an imaging system is presented in the following sections.

3. Sensitivity Measurement

Using an image of colored chart, a system of linear algebraic equations could be written for estimation of the spectral sensitivities of the camera. Taking transpose from both side of Equation 2 and solving \mathbf{W}_L for each camera channel leads to a linear system of equations as shown in Equation 4.

$$\mathbf{R}^t \mathbf{W}_{L,i} = \mathbf{c}^t, i = 1, \dots, n_c \quad (4)$$

Where \mathbf{R} and n_c denote the matrix of reflectances and the number of camera channels, respectively.

It was shown in many literatures [9-12] that a few basis vectors can cover most of the reflectance databases. This shows that the singular values are approximately zero for other dimensions which itself causes Equation 4 to be an ill-posed problem. Solving this equation using simple pseudo-inverse solution will result in spiky answer. The smooth behavior of the sensitivity curves of the imaging sensors is a good criterion for solving the problem of sensitivity estimation. Thus, a simple solution is to avoid singular values that are close to zero. This would eliminate the role of the last Eigen vectors which cause fluctuations in the answer. This technique, called truncated singular value decomposition (T-SVD), has been fully reviewed by Hansen [13]. By using singular value decomposition of \mathbf{R} , the answer of Equation 4 could be written as Equation 5.

$$\mathbf{W}_{L,i} = \sum_{j=1}^{n_i} \kappa_j \mathbf{v}_j; \text{ where } \kappa_j = \frac{\mathbf{u}_j^t \mathbf{c}_i}{\sigma_j}, \quad (5)$$

$$\mathbf{R} = \sum_{j=1}^{n_r} \sigma_j \mathbf{u}_j \mathbf{v}_j^t, i = 1..n_c, n_i \leq n_r.$$

Where n_r and n_t are the rank of the reflectance of \mathbf{R} and truncation point of T-SVD technique, respectively. σ , \mathbf{u} , \mathbf{v} are singular value, left and right basis vectors of singular value decomposition (SVD) of reflectance matrix of \mathbf{R} . It should be emphasized that the only way to control the accuracy of estimation of sensitivities is the direct measurement of the sensitivities [14, 15] or inquiring from the manufacturer.

4. Noise

Noise is an indivisible part of an imaging system. It can be regarded as uncertainty of the imaging device signals. Although noise is divided into two signal dependent and independent parts, it is common to only assume the signal dependent part which is correlated to the signal by a signal to noise ratio (SNR) as defined in Equation 6 [4, 16, 17].

$$SNR = 10 \log_{10} \left(\frac{\text{trace}(\mathbf{W}_L' \mathbf{K}_r \mathbf{W}_L)}{\text{trace}(\mathbf{K}_n)} \right) \quad (6)$$

If noise is white, then

$$\mathbf{K}_n = \sigma_n^2 \mathbf{I} \quad (7)$$

And for a given SNR, noise variance is calculated as:

$$\sigma_n^2 = \frac{\text{trace}(\mathbf{W}_L' \mathbf{K}_r \mathbf{W}_L)}{n_c \times 10^{\frac{SNR}{10}}} \quad (8)$$

For a real camera, noise variance is calculated using Equation 9.

$$\sigma_n^2 = \frac{1}{n_c} E \left(\text{trace} \left((\mathbf{c} - \mathbf{W}_L' \mathbf{r})' (\mathbf{c} - \mathbf{W}_L' \mathbf{r}) \right) \right) \quad (9)$$

In practice, using Equations 6-8 and assuming white, Poisson distributed noise of the imaging system; noise with a definite SNR could be generated. This noise could be used in modeling of imaging systems. It is worth noting that although \mathbf{K}_r entered into Equation 6, this does not mean that SNR of the imaging system depends on the dataset. In other words, SNR represents the ratio of signal power to the noise power in the logarithmic scale and some mathematical substitution of this notion and some simplifications result in Equation 6. The accuracy of the estimated noise variance depends directly to the accuracy of the

sensitivity and assumptions in modeling of noise.

5. Geometrical model of the idea

It was shown in [3] that the necessary and sufficient condition for having minimum error reflectance estimation is to cover the range of the reflectances by the illumination weighted sensitivities of the camera as shown in theorem 10.

$$\mathcal{R}(\mathbf{R}) \subseteq \mathcal{R}(\mathbf{W}_L) \Leftrightarrow E(\mathbf{e}_{spectral}) \quad (10)$$

is the minimum possible value independent of \mathbf{K}_r

where, \mathcal{R} denotes the range of columns of a matrix. E is the expected value operator and $\mathbf{e}_{spectral}$ is the spectral estimation error vector.

Now we are going to rearrange theorem 10 in another way but before that let's rephrase the current theorem. If \mathbf{R} is written as $\mathbf{R} = \mathbf{P}_B \mathbf{B}$, where \mathbf{B} is a set of basis for the reflectance set of \mathbf{R} and \mathbf{P}_B is the projector operator onto \mathbf{B} , then theorem 10 can be rewritten as:

$$\mathcal{R}(\mathbf{P}_B) \subseteq \mathcal{R}(\mathbf{W}_L) \Leftrightarrow E(\mathbf{e}_{spectral}) \quad (11)$$

is the minimum possible value independent of \mathbf{K}_r

This means that for having minimum error prediction of reflectances from the camera responses it is necessary and sufficient that the range of the projector operator onto the targeted subspace be a subset of the illumination weighted sensor subspace.

In vector space point of view, tristimulus prediction means seeking projection onto the CIE color matching functions, that is the fundamental metamers [2, 18, 19]. This implies that theorem 11 could be rewritten as

$$\mathcal{R}(\mathbf{P}_{CMF_L}) \subseteq \mathcal{R}(\mathbf{W}_L) \Leftrightarrow E(\mathbf{e}_{colorimetric}) \quad (12)$$

is the minimum possible value independent of \mathbf{K}_r

where, \mathbf{CMF}_L is the illumination weighted color matching functions and $\mathbf{e}_{colorimetric}$ is the difference between fundamental metamers. Theorem 12 gives valuable criterion for the sensors of a RGB or a multichannel camera, i.e. illumination weighted color matching functions should be fully spanned by the illumination weighted sensitivities of the camera in order to have the lowest possible colorimetric error. It should be noted that the colorimetric error arises from two factors. The first is the lack of covering the

weighted color matching function and the second is the noise of the imaging system that diverts the projection location from its true position [20, 21]. Equation 12 has been driven previously by Vora et al. for a noiseless imaging scanner [2]. For a noisy imaging system, a spectral metric based on spanning of subspaces was developed [3]. Equation 12 is the colorimetric representation of this spectral metric.

The geometrical illustration of Equation 12 is shown in Figure 1. In this figure, \mathbf{r} is a random vector selected from data set. $\mathbf{W}_{L,1}$ and $\mathbf{W}_{L,2}$ are two sensor-illumination sets. The true tristimulus value of \mathbf{r} is OB , which is the projection of \mathbf{r} onto \mathbf{CMF}_L . The estimation of the tristimulus values via response of the imaging systems 1 and 2 are OC and OE and the corresponding estimation errors are CB and EB . It can be seen that the prediction of tristimulus values via $\mathbf{W}_{L,1}$ gives lower error comparing to $\mathbf{W}_{L,2}$. This is because the angles between $\mathbf{W}_{L,1}$ and \mathbf{CMF}_L are very small comparing to the angle between $\mathbf{W}_{L,2}$ and \mathbf{CMF}_L . In fact, lower angle means better spanning as it has been shown in ref [2, 3].

Although the current rationale justifies reconstruction via simple projection, as it has been shown in ref [3] it is quite applicable for the well-known wiener estimation technique. However, the geometrical illustration would not be as simple as show in Figure 1, and needs deep understanding of the mechanism of the estimation method. The noise of the imaging system will result in deviation of projection point from its location depending of the SNR of the system. The uncertainty due to the noise is shown with parenthesis on $\mathbf{W}_{L,1}$ and $\mathbf{W}_{L,2}$ axes.

6. Experimental

A. Imaging system setup

A Canon Kiss X3 camera was used for implementation of the proposed algorithm. According to the device specifications, the camera gives 14 bit raw images. Raw format was used for the shots. Using an open source program, named dcrw [22], raw shoots were developed under linear gamma and 16 bits digital quantization level. No image compression was used in developments. Using 12 central gray patches of Gretag Macbeth Color Checker[®] DC (CCDC), it was seen that the camera is acceptably linear for its all 3 channels. Using a white card, vignetting and non-uniformity of illumination was corrected. Natural light of noon daylight on a sunny day was used for the illumination. In order to have the same

viewing/measurement geometry, reflectances of the chart's color patches were measured using GretagMacbeth Color Eye 7000 spectrophotometer.

B. Spectral sensitivity measurement

CCDC color chart was used for estimating the spectral sensitivities of the camera. It has been shown [4] that maximizing the colorimetric characteristic of the sensitivities is a good criterion for choosing the number of singular values. Sensitivities of the camera channels have been measured using T-SVD method and choosing 6, 5 and 5 first singular values for red, green and blue channels.

The use of simulated camera signals instead of real camera seems unrealistic at first glance; it has the advantage of avoiding manufacturing real filters. Although it has been shown that filters could be optimized considering their constructability [4], this would even have some drawbacks including limiting the filters to the color primaries spectral gamut and the spatial defects of the physical filters.

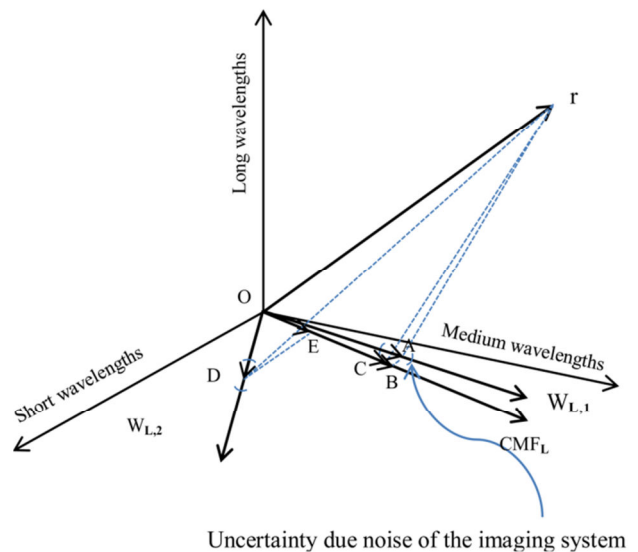


Figure 1: Illustration of spectral and colorimetric estimation of an imaging system using simple projection method.

C. Filter design and optimization

Optimizing the filter spectral transmission necessitates minimizing prediction errors. As there are many wavelengths to be optimized, numeric optimizations may get stuck in local optima. Moreover, the optimized answer may not have the reasonable transmission of an available optical filter. In order to solve this problem, sum of two Gaussian functions has been used to reduce the optimization parameters. This is shown in Equation 13.

$$y = a_1 \exp\left(-\left(\frac{x - \mu_1}{\sigma_1}\right)^2\right) + a_2 \exp\left(-\left(\frac{x - \mu_2}{\sigma_2}\right)^2\right). \quad (13)$$

In fact, filter spectral transmission is modeled by just six parameters of a_1 , a_2 , μ_1 , μ_2 , σ_1 and σ_2 . The proposed function not only has the advantage of reducing the optimization parameters to 6, also it can model transmission of many available optical filters [23]. To the best of the author's knowledge, it is common to use up to 2 filters for spectral estimation using RGB cameras [24-27] and rarely, if ever, more than two filters has been used. So, two methods were used for designing the filters. The first method was to leave the camera unchanged and designing the other filter for using with the first one to make a 6-channel camera. The other method was to optimize two filters for using in front of camera lens to make spectral camera. Optimization was performed using Genetic Algorithm. Migration, Crossover and Mutation fractions were adjusted to 20%, 70% and 10%, respectively. Population size was assumed to be 100. Stopping criteria was adjusted such that optimization continues up to 100 generations or change in the best fitness function value over Stall generations is less than or equal to 1E-6.

Among spectral and colorimetric metrics [2, 21, 28], the one that proposed by Mahmoudi et al. as "Modified Measure of Goodness" (MMOG) was selected as fitness function. MMOG is completely a spectral based metric which takes noise into account and is based on the spanning of subspaces as shown in Equation 14 [3].

$$MMOG = \frac{\text{trace}\left(\mathbf{P}_B \left(2\mathbf{K}_r \mathbf{P}_{W_L} - \mathbf{Q}_{W_L} \left(\mathbf{W}_L \mathbf{K}_r \mathbf{W}_L + \mathbf{K}_n\right) \mathbf{Q}_{W_L}'\right)\right)}{\text{trace}\left(\mathbf{P}_B \mathbf{K}_r\right)}. \quad (14)$$

Where \mathbf{P}_B is the projector matrix onto basis vectors

of the dataset, $\mathbf{Q}_{W_L} = \mathbf{W}_L \left(\mathbf{W}_L' \mathbf{W}_L\right)^{-1}$ and $\mathbf{P}_{W_L} = \mathbf{W}_L \left(\mathbf{W}_L' \mathbf{W}_L\right)^{-1} \mathbf{W}_L'$. MMOG is a metric for evaluation of filter set in terms of RMSE of error. It varies between 1 for the best filter set and 0 for the worst one. The optimization algorithm seeks to minimize 1-MMOG.

As shown in [3], filter optimization using spectral metric will have infinite set of answers each has spanned equally the dataset. The same was also observed here. The optimizations end in different answers with comparable performance. Moreover, the randomness of selecting the train and test samples results in different solutions. So, each optimization was repeated 10 times to avoid getting stuck in local minima, premature convergences and the effect of training and testing datasets.

D. Datasets

Three datasets were used for checking the proposed idea. The first was 1269 Munsell matt data set, the second was color checker DC with 180 samples and the third dataset was a 512x512x31 spectral image consists of images of colorful Beads with some gray and colored patches of Macbeth 24 patches color checker chart. The rendered image of spectral image in Srgb color space is shown in Figure 2. For each data set, the first randomly-selected half of the samples was used for estimation of covariance matrix and the other half was used for the tests. Moreover, in order to study the cross dataset effect on the proposed idea, Munsell data set was considered as training set and the Beads dataset was considered as test. This combined state was named as Cross.



Figure 2: Beads.

E. Simulated noisy imaging data

The noise variance of the camera was estimated using Equation 9 and the SNR of the imaging system was estimated using Equations 6 and 7. Using the estimated noise variance of the camera, the responses of the camera to Munsell and CCDC color patches, which are calculated using Equation 2, were contaminated with noise.

i. From Equation 8, variance of noise for a given SNR was calculated.

ii. Using a Poisson random generator matrix of Poisson-distributed noisy numbers ($\mathbf{X}_{n_c \times n_s}$) was generated. The subscripts are the dimensions of \mathbf{X} , and n_s is the number of samples.

iii. $\mathbf{X}_{n_c \times n_s}$ is centered around its mean using Equation 15.

$$\mathbf{X}_{centered} = \mathbf{X}_{n_c \times n_s} - \bar{\mathbf{X}}_{n_c \times 1} \times \begin{bmatrix} 1 & \dots & 1 \end{bmatrix}_{1 \times n_s} \quad (15)$$

iv. As the covariance matrix of the noise is not an Identity matrix, \mathbf{A} is converted to $\mathbf{X}_{centered}$ using transformation \mathbf{Y} as shown in Equation 16.

$$\mathbf{Y} = \mathbf{A}\mathbf{X}_{centered}, \mathbf{A} = \mathbf{\Lambda}_X^{-\frac{1}{2}}\mathbf{\Phi}_X^t, \mathbf{K}_X = \mathbf{\Phi}_X\mathbf{\Lambda}_X\mathbf{\Phi}_X^t \quad (16)$$

In Equation 16, $\mathbf{\Lambda}_X$ is diagonal matrix of Eigen values and $\mathbf{\Phi}_X$ is the matrix of Eigen vectors of the

matrix \mathbf{X} .

v. As covariance matrix of the matrix of \mathbf{Y} is \mathbf{I} [29], the matrix \mathbf{Y} is multiplied by σ_n so as to change its covariance matrix to a diagonal matrix with σ_n^2 on the main diagonal.

vi. Camera responses are added to \mathbf{Y} values to get the noisy camera responses with white noise and definite SNR. Noises were added in different SNRs to the simulated camera responses.

7. Results and Discussion

Spectral sensitivities of camera 3 channels are shown in Figure 3. The estimated SNR of the imaging system using the described method in the experimental section was about 35. This level of SNR was acquired using imaging of CCDC such that each color patches contain 37*37 pixels.

Vora’s measure of goodness for the sensitivities was measured as 0.9172 which means 23.5 degrees of divergence from human visual subspace (HVSS) which means small deviation from color matching functions subspace. This shows that the studied camera satisfies to some extent “Luther condition”. So, according to section 5, it would be a wise idea to take account of these sensitivities in modeling of the imaging system. Different scenarios of filter design were studied.

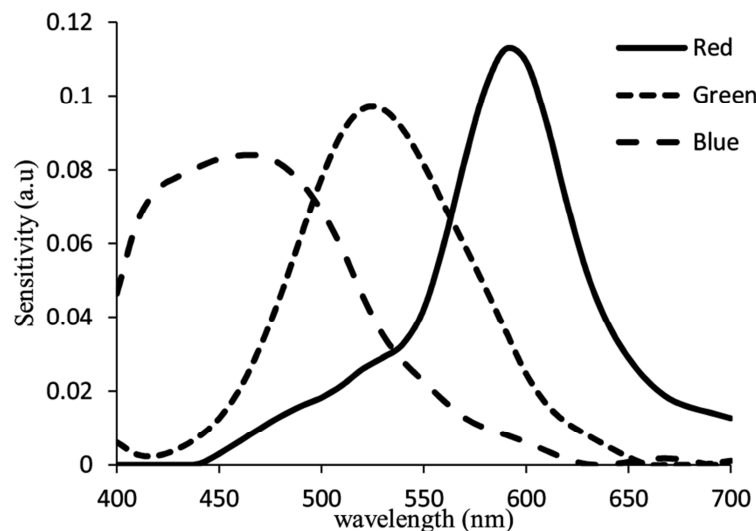


Figure 3: Spectral sensitivities of canon kiss X3 channels.

A. Canon Kiss X3: The original sensitivities+1 filter Vs. 2 filters

Assuming Canon kiss X3 as sensor, camera signals were calculated using Equation 2. White noise variance was calculated using Equation 8. Afterwards, noise was generated using the six steps explained in section 6E. Then the noise was added to the camera signals to develop camera noisy signals.

Filters were optimized by minimizing Equation 14. Filters supposed to be modeled using Equation 13 and the 6 and 12 parameters were optimized for one and two filters, respectively. The 3 datasets and the Cross dataset were used in the optimization. Results are shown in Table 1.

As can be seen from Table 1, imaging with 2 filters enhanced the performance of spectral estimations (probably meaningful for DC and Munsell and significantly for Beads dataset). Meanwhile, the colorimetric performance does not show significant improvement. This implies the deviation from HVSS after mounting 2 filters in front of the camera lens. In "1 filter+camera sensors" mode, despite our expectation colorimetric performance does not show improvement probably due to the 23.5 degrees of deviation from HVSS. This will be discussed in more detail in the next section.

In "2 filters" mode, the optimizer has enough freedom to search for better spanning the datasets, but not necessarily has the ability to span color matching functions. This could be attributed to the inherent fluctuations of Gaussian functions in Equation 13 which deviate the filter-sensor subspace from HVSS in

vector space point of view. This will be studied more in the next sections.

For the Cross dataset, both colorimetric and spectral performances do not improve in 1 filter setup indicating statistical difference of Munsell and Beads datasets. Using 2 filters has enabled system for better spanning Beads dataset.

B. Completely colorimetric camera: The original sensitivities+1 filter Vs. 2 filters

It was also assumed that the camera possesses complete colorimetric behavior. Camera signals were contaminated with noise using the procedure explained in section 7-A. Filters were optimized and the reflectances of the test samples were estimated using Equation 3. Results are shown in Table 2.

As could be seen in Table 2, while the colorimetric performance has been remained unchanged for DC dataset, it has increased significantly for Munsell and Beads datasets and also cross dataset case in 1 filter+camera sensitivities mode. However, there is clear contrast between RMSE trends and color differences. RMSE values for all datasets have been significantly decreased in "2 filters" mode at least for the Beads data set and the Cross case.

Comparison of Table 1 with Table 2, shows completely reverse trend between spectral and colorimetric metrics. In Table 1, optimizing using two filters has improved spectral and colorimetric performances while in Table 2, colorimetric performances decrease despite improvement of RMSE.

Table 1: Colorimetric and spectral performance of canon kiss X3.

Data set	Metric	1 filter+camera sensors		2filters	
		Average	Max	Average	Max
DC	RMSE	0.0185±0.0012*	0.0402	0.0157±0.0014	0.0336
	$\Delta E_{D65/10^0}^*$	3.35±0.60	11.18	3.32±0.63	11.32
Munsell	RMSE	0.0138±0.0005	0.0351	0.0128±0.0006	0.0323
	$\Delta E_{D65/10^0}^*$	2.76±0.24	10.28	2.73±0.21	8.95
Beads	RMSE	0.0129±0.0003	0.0377	0.0111±0.0002	0.0300
	$\Delta E_{D65/10^0}^*$	3.25±0.06	8.24	3.15±0.07	7.83
Cross	RMSE	0.0243±0.0002	0.0604	0.0205±0.0001	0.0565
	$\Delta E_{D65/10^0}^*$	5.09±0.05	11.82	3.91±0.03	8.50

*Uncertainties are 2 times of standard error of predictions.

This interesting reverse trend could be related to the spectral reflectance of the real objects which rarely possess 3 humps in their shape like color matching functions. In other words, although entering color matching functions as basis functions into reconstructions has the advantage of spanning HVSS, it may put distance between spectral reflectance subspace and the camera sensors.

Comparison of these two tables in similar scenarios is also informative. Making the Canon Kiss X3 colorimetric but with the same noise features enhances color difference significantly specifically for “1 filter + camera sensors” categories supporting the proposed idea of the current study. It was easy to notice that RMSE decrease were not significant in most of the cases in section 7-A. The remarkable improvement in colorimetric performance may contribute to the colorimetric behavior of the sensors. In other words, as it was shown in Equation 12, covering color matching functions by filters vectors guarantees minimum possible error in tristimulus values and their predictions. Despite considerable improvement in “1 filter + camera sensors” scenario, there still remained color differences. We believe that the considerable color differences in Table 2 are due to the noise of the imaging system which is studied in the next section.

C. Completely noiseless colorimetric camera: The original sensitivities+1 filter Vs. 2 filters

In order to study the remained color differences for the

case of “1 filter +camera sensors” in section 7-B, SNR was assumed to be infinite. Using the same datasets, the performance of the imaging system was studied for the optimized “filter+ camera” sensors and also for a set of 2 filters. Results are shown in Table .

It can be seen from Table that the color difference metric is almost zero for all data sets, while there is no significant difference between spectral performances. This proves the claim in section 5.

These findings are in close match with the work published by Trussell et al. [30]. It was reported that in the absence of noise, the selection of filters for covering the span of illumination weighted color matching functions gives the best colorimetric performance. However, the result got worse as noise entered in the system probably due to the noise sensitivity of imaging system as it gets away from mutual orthogonality of the channels [3].

In case of Cross dataset, in our all 3 studies scenarios, as it was expected, results showed significantly higher colorimetric and spectral performance compared to the Munsell and Beads cases. It should be noticed that these colorimetric performances achieved using optimization of MMOG metric - that had no guarantee for colorimetric performance - resulted in superior colorimetric performance.

Table 2: Colorimetric and spectral performance of a colorimetric camera.

Data set	Metric	1 filter +camera sensors		2filters	
		Average	Max	Average	Max
DC	RMSE	0.0187±0.0018*	0.0390	0.0167±0.0017	0.0373
	$\Delta E_{D65/10^0}^*$	2.99±0.69	11.00	3.08±0.54	10.07
Munsell	RMSE	0.0142±0.0011	0.0378	0.0130±0.0007	0.0358
	$\Delta E_{D65/10^0}^*$	2.00±0.16	6.41	2.38±0.19	9.02
Beads	RMSE	0.0138±0.0003	0.0391	0.0117±0.0002	0.0343
	$\Delta E_{D65/10^0}^*$	2.31±0.04	5.42	2.62±0.04	6.43
Cross	RMSE	0.0246±0.0002	0.0720	0.0203±0.0002	0.0587
	$\Delta E_{D65/10^0}^*$	3.93±0.03	9.33	4.43±0.04	9.98

*Uncertainties are 2 times of standard error of predictions.

Table 3: Colorimetric and spectral performance of a colorimetric noiseless camera.

Data set	Metric	1 filter +camera sensors		2filters	
		Average	Max	Average	Max
DC	RMSE	0.0086±0.0012*	0.0218	0.0095±0.0014	0.0386
	$\Delta E_{D65/10^0}^*$	0.00±0.00	0.01	0.89±0.20	1.87
Munsell	RMSE	0.0067±0.0004	0.0213	0.0072±0.0004	0.0257
	$\Delta E_{D65/10^0}^*$	0.00±0.00	0.01	0.47±0.05	2.31
Beads	RMSE	0.0079±0.0002	0.0235	0.0077±0.0002	0.0217
	$\Delta E_{D65/10^0}^*$	0.01±0.00	0.03	0.54±0.01	3.10
Cross	RMSE	0.0198±0.0002	0.0586	0.0273±0.0002	0.0709
	$\Delta E_{D65/10^0}^*$	0.02±0.00	0.05	3.42±0.03	7.71

*Uncertainties are 2 times of standard error of predictions.

8. Conclusion

It was shown that RGB cameras can take advantage of their inherent colorimetric characteristic in spectral imaging. In cameras with close-to-colorimetric behavior, it would be a good idea to take in to account their sensitivities as set of camera channels for spectral estimation. Embedding camera data, which is taken with bare lens into the filter equipped data, not only can enhance the colorimetric behavior of the imaging system, but also preserve its spectral performance. It was seen that adding a shoot with a bare lens for a complete colorimetric noiseless camera is a necessity that cannot be avoided. It is worth noting that, because of signal-independent parts of noise of imaging systems, SNR value

decreases as signal decreases. This was not assumed in this paper for simplicity of the modeling. Bare lens shoot can have the advantage of increasing the total SNR of the imaging system in practice. Although spectral estimation using filter-equipped cameras need a reconstruction technique for estimation and almost all of the methods need some sort of training database, the presented technique theoretically enhances the colorimetric performance of the reconstructions regardless of the training dataset. Spectral estimation using camera data need a reconstruction technique for estimation. In this study, Wiener filter technique was used. The combination of other reconstruction method with the proposed idea could be the subject of future studies.

5. References

1. F. Martínez-Verdú, J. Pujol, P. Capilla, Characterization of a Digital Camera as an Absolute Tristimulus Colorimeter, *J. Imaging Sci. Technol.*, 47(2003), 279-295.
2. P. L. Vora, H. J. Trussell, Measure of goodness of a set of color-scanning filters, *J. Opt. Soc. Am. A*, 10(1993), 1499-1508.
3. A. Mahmoudi Nahavandi, M. Amani Tehran, Metric for evaluation of filter efficiency in spectral cameras, *Appl. Opt.*, 55(2016), 9193-9204.
4. A. Mahmoudi Nahavandi, M. Amani Tehran, A new manufacturable filter design approach for spectral reflectance estimation, *Color Res. Appl.*, 42(2016), 316-326.
5. A. Mahmoudi Nahavandi, M. Amani Tehran, Image-based spectral transmission estimation using sensitivity comparison, *Appl. Opt.*, 56(2017), 417-423.
6. R. S. Berns, L. A. Taplin, M. Nezamabadi, Spectral imaging using a commercial color-filter array digital camera, in The Fourteenth Triennial ICOM-CC meeting, The Hague, Netherlands, (2005), 743-750.
7. S. Tsutsumi, M. R. Rosen, R. S. Berns, Spectral color management using interim connection spaces based on spectral decomposition, *Color Res. Appl.*, 33(2008), 282-299.
8. W. K. Pratt, *Digital Image Processing*, 3rd Edition ed., John Wiley & Sons, Los Altos, California, 2001, 356-365.
9. D. Connah, S. Westland, M. G. A. Thomson, Recovering spectral information using digital camera systems, *Color. Technol.*, 117(2001), 309-312.
10. E. M. Valero, J. L. Nieves, S. M. C. Nascimento, K. Amano, D. H. Foster, Recovering spectral data from natural scenes with an RGB digital camera and colored filters, *Color Res. Appl.*, 32(2007), 352-360.

11. S. G. Kandi, Spectral Estimation of Printed Colors Using a Scanner, Conventional Color Filters and Applying Backpropagation Neural Network, *Prog. Color Colorants Coat.*, 4(2011), 39-50.
12. R. Jafari, S. H. Amirshahi, Spectral Reconstruction of Blacks and Whites by Using the Statistical Colorants *Prog. Color Colorants Coat.*, 8(2015), 135-144.
13. P. C. Hansen, Regularization Tools, A Matlab Package for Analysis and Solution of Discrete Ill-Posed Problems, T. U. o. D. Informatics and Mathematical Modelling Building 321, DK-2800 Lyngby, ed. Denmark, (2008).
14. S. Han, Y. Matsushita, I. Sato, T. Okabe, Y. Sato, Camera spectral sensitivity estimation from a single image under unknown illumination by using fluorescence, in 2012 IEEE Conference on Computer Vision and Pattern Recognition, (2012), 805-812.
15. J. Jiang, D. Liu, J. Gu, S. Süssstrunk, What is the space of spectral sensitivity functions for digital color cameras?, in 2013 IEEE Workshop on Applications of Computer Vision (WACV), FL, USA, (2013), 168-179.
16. A. Mahmoudi Nahavandi, Noise segmentation for improving performance of Wiener filter method in spectral reflectance estimation, *Color Res. Appl.*, 43(2018), 341-348.
17. H. Kuniba, R. S. Berns, Spectral sensitivity optimization of color image sensors considering photon shot noise, *J. Electronic Imag.*, 18(2009), 1-14.
18. J. B. Cohen, W. E. Kappauf, Metameric Color Stimuli, Fundamental Metamers, and Wyszecki's Metameric Blacks, *American J. Psychol.*, 95(1982), 537-564.
19. J. B. Cohen, W. E. Kappauf, Color Mixture and Fundamental Metamers: Theory, Algebra, Geometry, Application, *American J. Psychol.*, 98(1985), 171-259.
20. G. Sharma, H. J. Trussell, Figures of merit for color scanners, *IEEE Transactions Image Proc.*, 6(1997), 990-1001.
21. D. Coffin, *Decoding raw digital photos in Linux* (2015), retrieved 28 November, 2015, <http://www.centrostudiprogressofotografico.it/en/dcrow/>.
22. E. Kodak, Kodak Filters for Scientific and Technical Uses, Eastman Kodak Co, USA, 1982, 1-94.
23. F. H. Imai, R. S. Berns, D.-Y. Tzeng, A Comparative Analysis of Spectral Reflectance Estimated in Various Spaces Using a Trichromatic Camera System, *J. Imaging Sci. Technol.*, 44(2000), 280-287.
24. D. C. Day, Filter Selection for Spectral Estimation Using a Trichromatic Camera, M.Sc., Rochester Institute of Technology Rochester, USA, 2003.
25. Y. Zhao, R. S. Berns, Image-based spectral reflectance reconstruction using the matrix R method, *Color Research & Application*, 32(2007), 343-351.
26. N. Du-Yong, J. P. Allebach, A subspace matching color filter design methodology for a multispectral imaging system, *IEEE Transactions on Image Processing*, 15(2006), 2631-2643.
27. S. Quan, N. Ohta, R. S. Berns, X. Jiang, Unified Measure of Goodness and Optimal Design of Spectral Sensitivity Functions, *Journal of Imaging Science and Technology*, 46(2002), 14.
28. K. Fukunaga, Introduction to Statistical Pattern Recognition, Second Edition ed., Morgan Kaufmann, San Francisco, CA, 1990, 30.
29. H. J. Trussell, A. Ö. Ercan, N. G. Kingsbury, Color filters: When "optimal" is not optimal, in 2016 IEEE International Conference on Image Processing (ICIP), Arizona, USA, (2016), 3987-3991.

How to cite this article:

A. Mahmoudi Nahavandi, Taking Full Advantage of RGB Sensor's Colorimetric Characteristics in Multi-Spectral Imaging. *Prog. Color Colorants Coat.*, 13 (2020), 121-130.

